

Research article

River stabilization reshaped human-nature interactions in the Lower Yellow River Floodplain



Chentai Jiao ^a, Xutong Wu ^{a,*}, Shuang Song ^a, Shuai Wang ^a, Bei Xiang ^a, Bojie Fu ^{a,b}

^a State Key Laboratory of Earth Surface Processes and Resource Ecology, Faculty of Geographical Science, Beijing Normal University, Beijing, 100875, China

^b State Key Laboratory of Urban and Regional Ecology, Research Center for Eco-Environmental Sciences, Chinese Academy of Sciences, Beijing, 100085, China

ARTICLE INFO

Keywords:

Human-nature interactions
The Lower Yellow River
Floodplains
River regulation

ABSTRACT

Floodplains are crucial agricultural and populated areas worldwide. Rivers typically shape human activities within floodplains through water supply and flood risk, forming unique human-nature interaction patterns. Given that river systems have undergone significant transformations globally, understanding the response of these interactions to hydrological changes is elementary. Here, using the Lower Yellow River Floodplain (LYRF) as a case, where continuous levees distinctly outline the river-influenced floodplain from a homogenous cultivated plain and the river's hydrology has undergone dramatic alterations since the 1990s, we analyzed how the human-nature interactions respond to river hydrological changes. This study found that the flood-prone nature of the Lower Yellow River has weakened from 1986 to 2021 as shown by decreased surface water extent and inundated extent of cropland. The intensity of agriculture inside the LYRF has been lower but experienced faster development than outside, minimizing the disparity between them. Meanwhile, human activities in the floodplain have moved closer to the river. These changes in human-nature interactions in the LYRF can be explained by the river stabilization caused by upstream regulation, underscoring the significance of integrated river governance in managing human-nature system in floodplain areas.

1. Introduction

Floodplains are low-lying lands bordering a river, comprised of sediment carried by the stream, defined by the perimeter of the maximum probable flood, and while typically dry, are subject to flood and river overflow inundation (Bryan, 1923; Hoyt and Langbein, 1955; White, 1945). Offering favorable conditions such as fertile soil, accessible water supply, and flat terrain, floodplains in lower reaches of large rivers have historically served as hubs for thriving ancient civilizations (Charloux et al., 2021; Mazzoleni et al., 2021; Tockner and Stanford, 2002). Today, these areas remain agriculturally important, hosting numerous settlements and a substantial population (Di Baldassarre et al., 2013a; Mazzoleni et al., 2021; Tockner and Stanford, 2002). However, living within floodplains carries an elevated risk of flooding compared to other areas. To mitigate and adapt to this risk, local communities have employed strategies such as constructing levees, planning cultivation strategically, and sometimes relocating from low-lying areas (Charloux et al., 2021; Dawson et al., 2011; Hino et al., 2017; Mazzoleni et al., 2021; Wang and Liu, 2019). As a result, a unique pattern of river-controlled human-nature interaction has evolved in floodplains,

where human response to the river's variation has a consequential impact on social productivity and stability (Di Baldassarre et al., 2013a; Mazzoleni et al., 2021). Understanding these interactions is crucial for effective floodplain management.

Human-nature interactions in floodplains or flood-affected areas have attracted scientific interest from various perspectives. Studies identifying human activities in the flood-affected areas has been conducted (Andreadis et al., 2022; Li et al., 2023; Rajib et al., 2023), as well as flood exposure estimation and projection (Devitt et al., 2023; Fang et al., 2021; Güneralp et al., 2015; Jongman et al., 2012; Tanoue et al., 2021; Wang et al., 2024). Anthropogenic influences, especially local measures within floodplains including human expansion and construction of levees, have been connected to flood risk and exposure (Ding et al., 2023; Schober et al., 2020). Studies have also revealed human response to flood in floodplains. Mitigation and adaptation measures, including structural measures (e.g., damming) and relocation (migration out of floodplain) have been analyzed in diverse regional scenarios (Aerts et al., 2024; Black et al., 2011; Bubeck et al., 2013; Devitt et al., 2023; Ding et al., 2023; Hino et al., 2017; Jongman et al., 2015; Wang et al., 2024). Further studies have delved into the driving forces behind

* Corresponding author.

E-mail address: wuxutong@bnu.edu.cn (X. Wu).

human response behaviors, with risk perception being emphasized (Di Baldassarre et al., 2013a,b; Rufat et al., 2015). Research suggests that human activity patterns in floodplains are based on collective memories of previous flood occurrences and changes in protection levels, indicating an increased protection level would promote development within floodplains (Barendrecht et al., 2019; Collenteur et al., 2015; Ding et al., 2023; Song et al., 2021). These social-hydrological feedback within flood-prone human-nature systems has been summarized by Di Baldassarre et al. (2013b) as a conceptional model (Di Baldassarre et al., 2013b, 2019). However, current studies usually consider local practices as the driving factor of human-nature interaction changes in floodplains, while hydrological changes' effect was less concerned. Secondly, commonly used human activity indicators including urban expansion, population and GDP are usually downscaled from global or statistical datasets, resulting in considerable uncertainty and limited resolution, which brings challenge to quantifying floodplain human activities, especially in terms of intensity. Therefore, there is a clear requirement for studies on floodplain human-nature interaction and its response to hydrological changes that incorporate long-term trend analysis and accurately quantified human activity patterns and intensity.

The Lower Yellow River Floodplain (LYRF) serves as a typical example of a dynamic floodplain human-nature system. Located in eastern China, the Lower Yellow River (LYR), which once frequently breached its banks and meandered across the North China Plain, has been confined within levees since the 1950s (Wang and Liu, 2019). These levees, engineered to withstand floods up to $2.2 \times 10^4 \text{ m}^3/\text{s}$, have successfully prevented breaches since their construction, thereby delineating the modern LYRF as a distinct region between the levees commonly known as the "Yellow River beach area" (Wang and Liu, 2019; Zhang et al., 2022). The local human-nature interaction, primarily characterized by an agricultural economy, has been fragile due to substantial flood risks. This vulnerability led to the government interventions such as population relocation to mitigate flood exposure. However, since the late 1990s, measures including the Grain for Green Program, reservoir construction, and unified basinal regulation have prompted a significant shift in the LYR's hydrology, featured by reduced discharge and sediment load since the late 1990s (Feng et al., 2016; Song et al., 2020, 2024; Wang et al., 2016, 2019; Yang et al., 2008). Such shifts have the potential to reshape human-nature interaction inside LYRF. Relevant research has explored governance strategies for LYRF social-ecological development (Zhang et al., 2022), evaluated and predicted habitat quality (Zhao et al., 2023), and quantified development levels using remote sensing methods (Li et al., 2023). Additional studies have described spatial patterns of agriculture and observed regime shifts in the human-river relationship (Run et al., 2022; Wu et al., 2023). While these studies have identified essential components of human-nature interaction, including river regulation, agriculture, ecology and land use change in LYRF, few have established connections among them or discussed the dynamics of their interactions under the hydrological changes of the Yellow River.

Therefore, the following hypothesis is proposed: as the river has stabilized in recent decades, human activity within the floodplain will be prompted and move closer to the river. To validate this hypothesis, this study embarks on a joint analysis on hydrological changes and human activities in the LYRF to probe the local human-nature interaction's response to riverine hydrological changes. Firstly, the study identifies the hydrological patterns of the LYR by utilizing remote sensing to extracted open-surface water bodies between 1986 and 2021. Secondly, human-nature interactions are represented with agricultural intensity, which is quantitatively assessed using Normalized Difference Vegetation Index (NDVI) on the cropland inside and around LYRF. The spatial patterns of human activities are then delineated, employing the physical distance from anthropogenic land use to river and the spatial distribution of agricultural intensity. Finally, a multiple correlation method is applied to identify potential relationships between hydrological and agricultural patterns. Through this approach, this research aims to

enhance the current understanding of hydrological influences on human-nature interactions, thereby providing scientific references for the management of the floodplain and the Yellow River Basin.

2. Method

2.1. Study Area

Spanning over 5400 km, the Yellow River is China's second-longest river, and its basin is the country's second-largest (Ringler et al., 2010). Upon leaving the Loess Plateau into the lower reach, the Yellow River deposits vast amounts of sediment, thereby elevating the channel by up to 20 m and forming a unique "hanging river", which is now constrained by the Yellow River Levees (Wu et al., 2023; Zhang et al., 2022). Located between the Yellow River Levees and the hilly regions of Shandong, the LYRF occupies this hanging river (Fig. 1). This study concentrates on the representative section of the floodplain, specifically the area between the Huayuankou and Lijin gauges, and the nearest levees adjacent to the river channel. The LYRF spans over 620 km and covering an area of 3200 km², with width varying from 500 m to 12 km (Fig. 1).

The LYR that shapes the LYRF is prone to flooding. With most of the basin located in arid or semi-arid zones and experiencing volatile monsoonal rainfall, the Yellow River exhibits intense inter- and intra-annual discharge variability (Jiao et al., 2023; Li et al., 2012; Wang and Sun, 2021; Xu and Ma, 2009). Furthermore, the river's middle reach traverses the Loess Plateau, a major soil erosion zone, leading to what was once the water body with the highest sediment load worldwide (Fu et al., 2017; Wang et al., 2016, 2017a). In the lower reach, sediment deposits silt up the channel, reducing its flood discharge capacity and causing frequent diversions within the LYRF (Wu et al., 2023). However, the Yellow River has undergone drastic water-sediment changes, with a 2/3 decrease in discharge and a nearly 90% reduction in sediment load over the past 60 years (Wang et al., 2016).

The LYRF encompasses a total of 37 counties within the provinces of Henan and Shandong, out of which 32 possess cultivated land exceeding 10 km² within the levees. 4 sub-regions, namely Henan-south (HnS), Henan-north (HnN), Shandong-south (SdS) and Shandong-north (SdN), are defined among these counties, with classification based on province and location relative to the riverbank (Fig. 1). These 32 counties comprise a population of 20.6 million, nearly 10% of the inhabitants, predominantly peasants, reside within the LYRF (Run et al., 2022). Owing to the temperate monsoon climate, irrigated winter wheat and summer maize are the dominant crops in LYRF and surrounding areas (Liu et al., 2010; Run et al., 2022). Presently, over 80% of the non-water area in LYRF (2500 km²) is cultivated, making the LYRF a hotspot for livelihood and food security.

The unique geography of LYRF presents an optimal quasi-natural experimental setting to evaluate the riverine flood impact on the human-nature interaction. Firstly, human-nature interactions in the LYRF are relatively straightforward, with cropland overwhelmingly dominating the floodplain. Since grains are the primary product of this interaction, serving as the most fundamental and impactful link in human-nature interactions (Wu, 1991), agriculture can be considered a fitting representation of the human-nature interactions in the LYRF. Secondly, the reinforced modern Yellow River Levees effectively eliminate the risk of riverine flood outside of them. Consequently, what was once a homogeneous cultivated plain is now divided into two sections, where nearly all factors contributing to agriculture, including climate, alluvial soil and administration, remain consistent across the levees, thus rendering the river the sole variable. Therefore, the impact of riverine floods on the human-nature interactions can be deduced by the differences in agriculture inside and outside the LYRF. Given that most other factors are naturally controlled, simple indices like NDVI can serve as proxies for agricultural input and output.

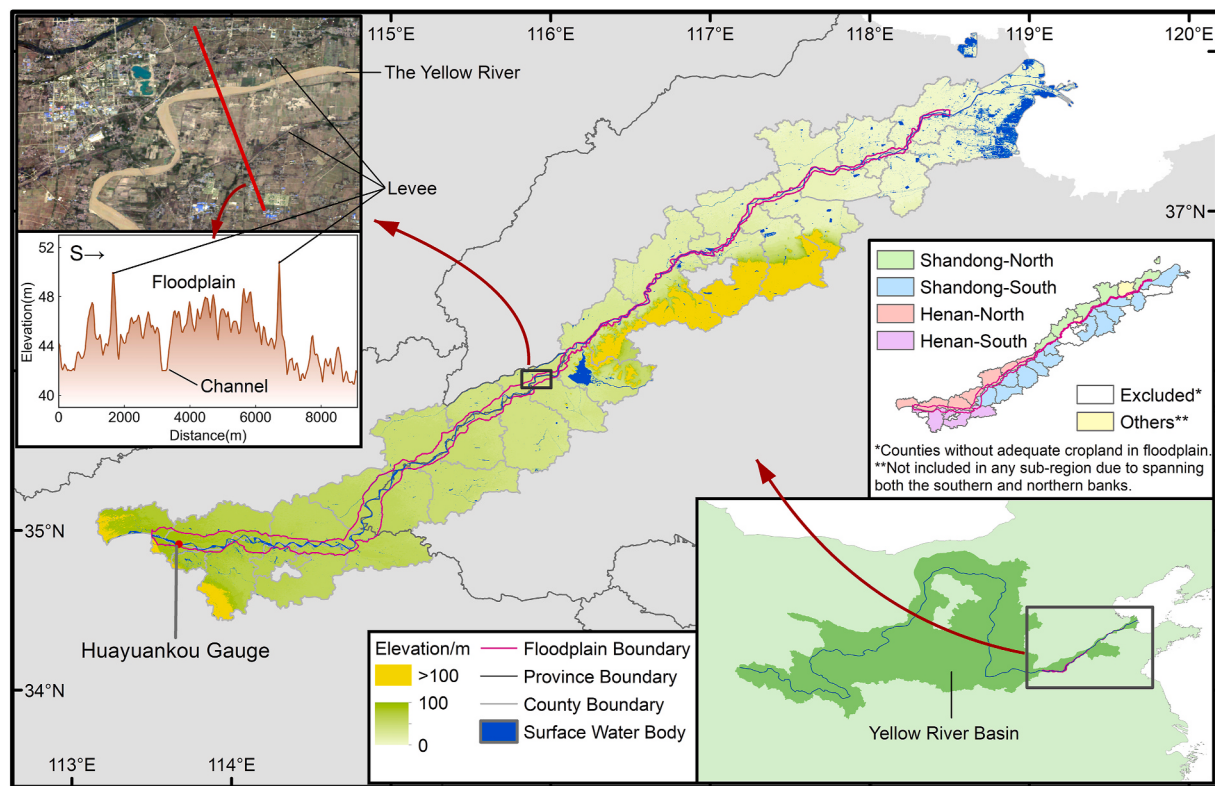


Fig. 1. Study area.

2.2. Water extraction and channel migration detection

This study uses open-surface water extent as the proxy of hydrological pattern of the LYR because it is a comprehensive variable for hydrological process and has immediate effect on human activity within the floodplain. This study utilizes the Google Earth Engine platform, Landsat series images, and a multi-indices algorithm comprising Modified Normalized Difference Water Index (MNDWI), NDVI, and Enhanced Vegetation Index (EVI) to extract open-surface water bodies in the LYRF from 1986 to 2021 (Deng et al., 2019; Jiao et al., 2023; Zou et al., 2017). The images employed for extraction include Landsat 5 TM, Landsat 7 ETM+, and Landsat 8 OLI surface reflectance images with atmospheric corrections applied (Fig. S1)(Schmidt et al., 2013). All tier 1 images available are utilized, except for Landsat 8 in 2013 due to its seasonal bias.

Firstly, invalid pixels are masked using a combined algorithm, where clouds and shadows are eliminated with the F-mask method (Zhu and Woodcock, 2012), and snow is removed by masking pixels with DN > 0.7 in all visible bands. Secondly, the following indices are calculated:

$$\text{MNDWI} = \frac{\text{G-SWIR}}{\text{G} + \text{SWIR}} \quad (1)$$

$$\text{NDVI} = \frac{\text{NIR} - \text{R}}{\text{NIR} + \text{R}} \quad (2)$$

$$\text{EVI} = \frac{2.5 \times (\text{NIR} - \text{R})}{\text{NIR} + 6 \times \text{R} - 7.5 \times \text{B} + 1} \quad (3)$$

Here, B, G, R, NIR, and SWIR represent the blue, green, red, near-infrared, and short-wave infrared (short-wave infrared 1 for Landsat 8) bands of the Landsat surface reflectance images. Water pixels are then extracted using the following condition:

$$\text{water} = \text{if } [\text{EVI} < 0.1 \text{ and } (\text{MNDWI} > \text{NDVI} \text{ or } \text{MNDWI} > \text{EVI})], 1, 0 \quad (4)$$

If the “water” variable returns 1, the pixel is defined as a water pixel (Zou et al., 2018). Then the historical maximum water bodies mask accessed from Joint Research Centre (JRC) global surface water database is applied to further improve the detection performance (Pekel et al., 2016). Subsequently, the water inundation frequency (WIF) of each pixel every year is calculated as:

$$\text{WIF} = \frac{\sum_{i=1}^N \text{water}}{N} \quad (5)$$

Here, “N” refers to the count of all good observations in a year. Pixels with WIF > 0.75 are defined as permanent water bodies, and those with WIF > 0.25 are defined as seasonal water bodies (Zou et al., 2017). Additionally, a maximum water extent is mapped with all pixels having WIF > 0 each year.

The stability of the river channel is quantified by migration rate of water bodies, which is calculated as the proportion of newly emerged water bodies in the total water bodies each year. A lower migration rate indicates a more consistent distribution of water bodies, suggesting higher river channel stability.

Cropland inundated extent in the LYRF is identified by combining the extracted open-surface water bodies with China’s annual cropland dataset (CACD)(Tu et al., 2023). Derived from Landsat images, CACD demonstrates superior accuracy compared to other commonly used cropland or Land Use/Cover data with similar spatial resolution and time series (Tu et al., 2023) and shares the same resolution with other datasets used in this study. For each year, a spatial overlay is conducted between cropland and seasonal/maximum water extent to define the area of intersection as seasonal/maximum inundated extent, respectively.

2.3. Quantification of intensity of agriculture

In this study, intensity of agriculture serves as an indicator of human

activity intensity in the LYRF. The quantification of this relies on the growing season NDVI on cropland, which is calculated using median-composite Landsat images acquired during May and September of each year, in alignment with crop schedule (Liu et al., 2010; Run et al., 2022). This NDVI is then masked and confined to cropland pixels obtained from CACD.

This study regards agriculture outside the levees as "normal" or unaffected by the river. To quantify the differences in agriculture between areas inside the LYRF and those outside, an "NDVI deficit" variable is used. The NDVI deficit is calculated at both the floodplain and county scales. At the floodplain scale, a 5 km buffer is established around the LYRF. For the county scale, the 32 counties with more than 10 km² of cropland within the LYRF are selected, as well as 4 sub-regions. The NDVI deficit is then calculated using the following formula:

$$\text{NDVI deficit} = \frac{\sum_{i=1}^N \text{NDVI}}{N} - \frac{\sum_{i=1}^n \text{NDVI}}{n} \quad (6)$$

Here, "N" and "n" refers to the total cropland pixels outside and inside the floodplain within the controlled area, respectively. "NDVI" refers to the NDVI during growing season on a pixel. A positive NDVI deficit indicates less flourishing agriculture within the LYRF than outside. The results are equally divided into three periods across the time series and averaged to demonstrate basic patterns, while concurrently conducting linear regression to detect possible trends.

2.4. Identification of spatial patterns of human activities

To identify spatial patterns of human activities, this study examines (a) the distance between anthropogenic land use and the river, and (b) the spatial distribution of agricultural intensity. In computing the anthropogenic-riverine distance, this study considers newly cultivated cropland and newly developed settlements. The former is determined from the CACD dataset with spatial erase tool in ArcGIS 10.7, while the latter is derived from the European Space Agency's World Settlement Footprint Evolution (WSFE) dataset. The WSFE dataset, also based on Landsat imagery, provides expansion record of settlements from 1986 to 2015 (Marconcini et al., 2020a,b). For distance analysis, the river is defined as permanent water bodies after manually discarding non-riverine water pixels. The distance is then calculated using the following formula:

$$\text{Distance} = \frac{\sum_{i=1}^N \text{EuD}}{N} \quad (7)$$

Here, N refers to the sum of selected pixels (newly cultivated cropland or newly developed settlements), and EuD refers to the Euclidean distance from river generated using the Euclidean distance tool in ArcGIS 10.7.

To illustrate the spatial distribution of intensity of agriculture, NDVI on cropland near the river is used for quantification. Initially, multiple buffer rings are established outside the river. Following this, the average NDVI on croplands within these buffer rings is computed, thereby generating a NDVI gradient from the river to the levees within LYRF. This gradient serves as an indicator of agriculture's sensitivity to its distance from river.

2.5. Time-series and inter-factor analysis

To establish links between hydrological change and floodplain agriculture variation, this study analyzes trends in the quantified variables over time series. A segmented linear regression method is applied to identify trends and potential turning points where changes in direction occur. Each year in the time series is considered as a potential turning point, as linear regressions being performed on both forward and backward segment that includes the turning point. The optimal turning point and regression are defined based on the following criteria.

- (1) Both segments must span at least 5 years, and their trends must be statistically significant to ensure the reliability of the regressions.
- (2) The regression coefficients of the two segments must have opposite signs, indicating a shift in the hydrological pattern.
- (3) The residual sum of squares is minimized among all regressions that meet criteria (1) and (2).

In the absence of a turning point, a linear regression is used for trend detection.

To further explore the impact of riverine hydrological change on human-nature interactions, a composite method comprising of both classical linear regression (CLR) based on null-hypothesis significance testing and Bayesian Linear Regression (BLR), is adopted. The analysis considers proxies of agriculture (NDVI deficit and NDVI gradient) as dependent variables and proxies of hydrological change (water body area, cropland inundation extent, and river channel stability) as influencing factors. The two regressions are conducted separately during the analysis.

CLR, which utilizes the least squares method, establishes a precise model between the selected variables. However, the use of p-values for model confidence assessment has drawn criticism due to issues such as the tendency to reject the null hypothesis with large datasets and interpretation challenges (Amrhein et al., 2019; Buchinsky and Chadha, 2017; Wakefield, 2009). Therefore, BLR is incorporated to further evaluate the potential relationship identified by CLR. BLR doesn't return an exact regression coefficient but rather provides a credible interval of regression coefficients for the chosen factors. It employs Bayes factor BF₁₀ to quantify evidence for H₁ (predictable model) relative to H₀ (non-predictable model) (van den Bergh et al., 2021). Unlike p-values, Bayes factors can be compared to show the interpretability of different models. For a thorough explanation of the method, can refer to van den Bergh et al., 2021. The confidence in CLR and the potential relationship are confirmed when

- (1) The classical regression coefficient falls within the credible interval generated with BLR.
- (2) The Bayes factor BF₁₀ is sufficiently large (BF₁₀ > 3 indicates Moderate evidence, BF₁₀ > 10 indicates Strong evidence and BF₁₀ > 100 for extreme evidence in support for H₁) (van den Bergh et al., 2021; Schönbrodt and Wagenmakers, 2018).

3. Results

3.1. Dynamic of open-surface water bodies

The extent and distribution of open-surface water bodies have exhibited significant changes since 1986 (Fig. 2a). The extent of permanent water bodies initially declined and then increased, with the turning point identified in 1999. In contrast, the maximum water extent initially increased, reaching its peak value of 749.9 km² in 2003, followed by a decrease after 2004. Seasonal water bodies exhibited a continuous decreasing trend of -1.59 km²/year. These changes in open-surface water bodies, particularly in seasonal and maximum water bodies, indicate a reduced flood intensity in the LYRB after the 2000s.

Simultaneously, the stability of the river channel has strengthened, as evidenced by reduced conversion rate between water and non-water states in the LYRF. The migration rate of seasonal water bodies decreased from 0.140 during 1987–1998 to 0.092 during 2010–2021 (Fig. 2b). The permanent water migration rate, which once reached 0.666 in 1996 (indicating 2/3 permanent water bodies in 1996 did not inherit from 1995), dropped by 0.238 between the same time periods. The decreased migration rate suggests that the LYR has displayed fewer wandering features and has transformed into regulated and settled channels.

The cropland inundation extent also exhibits consistent change patterns with open-surface water bodies (Fig. 2c). Seasonal inundated

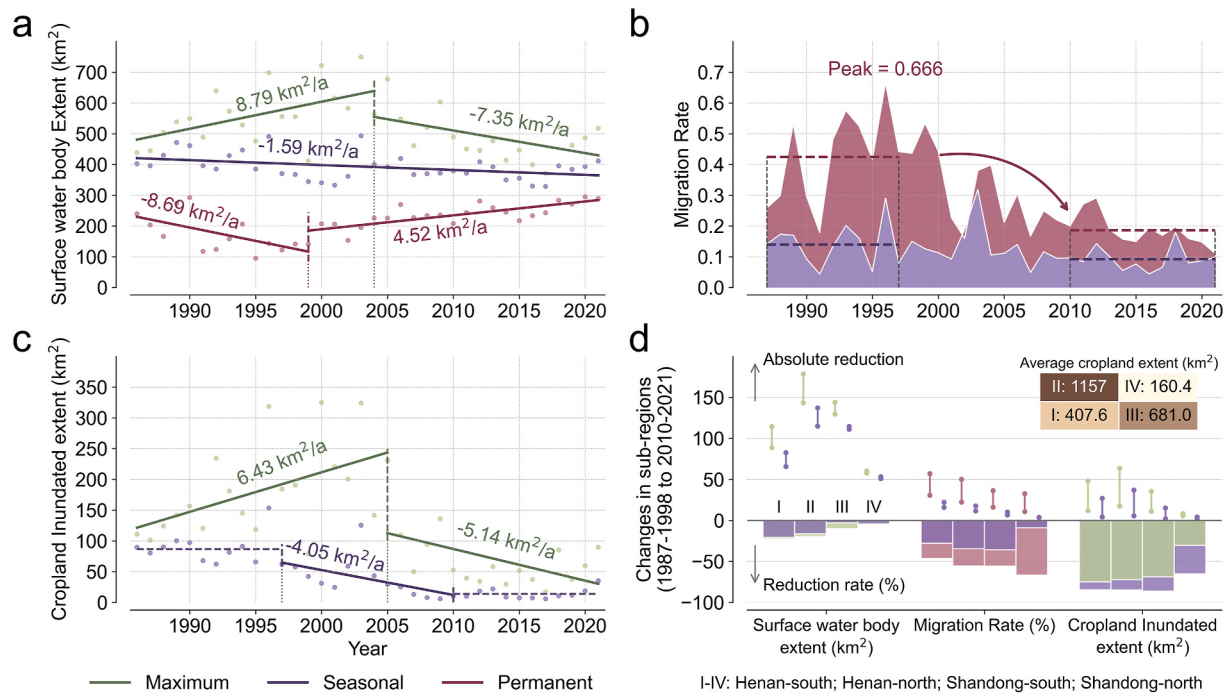


Fig. 2. Proxies of hydrological patterns in the LYRF. (a) The extent of open-surface water bodies. **(b)** Water body migration rate. **(c)** Cropland Inundated extent. **(d)** Changes of proxies in 4 sub-regions from 1987 to 1998 to 2010–2021.

extent has experienced a continuous decline, displaying comparatively high values before 1996, a sharp decline in the 2000s, and maintaining at a lower level during the 2010s. Maximum inundated extent shows a

trend of increase followed by decrease, with the turning point identified in 2005. Both types of inundated extent show a robust correlation with corresponding water body extents, with correlation coefficients being

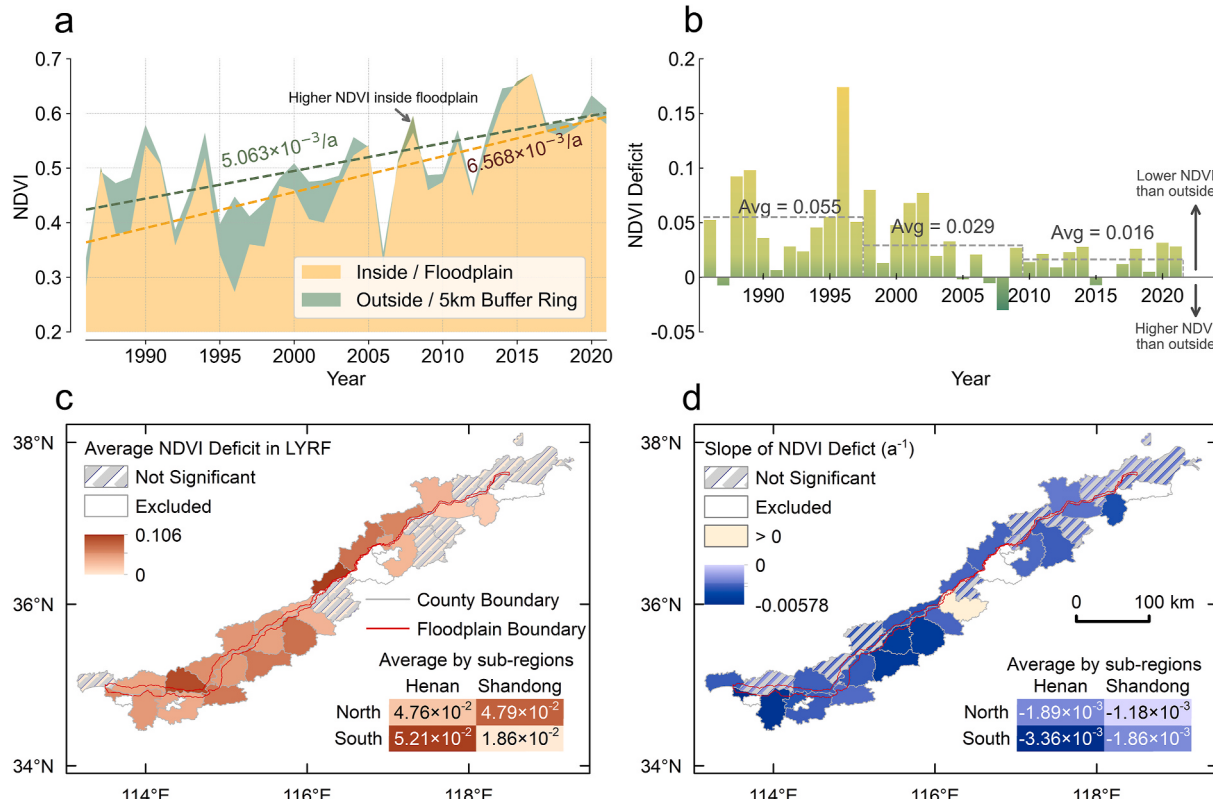


Fig. 3. NDVI variation in and around the LYRF. (a) Absolute cropland NDVI in the LYRF and in its outside buffer ring. **(b)** NDVI deficit in the LYRF. **(c)** NDVI deficit at the scale of county. **(d)** Tendency of NDVI deficit at the scale of county. (Excluded counties do not obtain enough cropland [10 km^2] in the LYRF and are not used for county-scale analyses).

0.93 and 0.77, respectively.

The pattern and dynamics of open-surface water bodies have displayed spatial heterogeneity (Fig. 2d). The HnN region has the largest surface water extent and cropland inundated extent among the four sub-regions. Yet in the HnS region with less cropland, the maximum cropland inundated extent reached 11.8% of total cultivated land during 1986–1997, compared to less than 6% in the other sub-regions. This indicates that the HnS region has been most seriously affected by flooding. However, from 1986 to 2021, the HnN and HnS have experienced a sharper decrease in seasonal and cropland inundated extent, while the Shandong regions was initially less inundated and experienced a milder reduction. However, the river migration rate in the SdN and SdS decreased rapidly. The permanent water migration rate of SdN has decreased by 67%, and seasonal water migration rate of SdS has decreased by 36% from 1986 to 1997 to 2010–2021, indicating a particular stabilization of the river channel in the lower reaches within the LYRF.

3.2. Increased intensity of agriculture in the LYRF

Intensity of agriculture within the LYRF, although initially lower, has rapidly increased, thereby narrowing the disparity between the LYRF and outside (Fig. 3a and b). At the floodplain scale, the average NDVI inside the floodplain is extremely significantly lower ($p < 0.001$) than that in the 5 km buffer outside during 1986–2021, with an average difference of 0.034. Nonetheless, the intensity of agriculture in the LYRF has progressively improved over time, with the average NDVI increasing at an average rate of 6.57×10^{-3} per year, faster than the neighboring region (Fig. 3a). As a result, NDVI deficit inside the floodplain have decreased at an average rate of $1.5 \times 10^{-3} \text{ year}^{-1}$ (Fig. 3b). The increased absolute NDVI and reduced NDVI deficit indicate an enhancement in agriculture within the LYRF. At the county scale, 24 out of the 32 available counties exhibit a significant NDVI deficit ($p < 0.05$) inside the floodplain, so do all 4 sub-regions (Fig. 3c, Fig. S2). The HnS

region that has been most severely inundated, also displays the highest NDVI deficit. The SdS region, which includes 4 of the 8 counties with insignificant NDVI deficit, exhibits a low NDVI deficit, which can be attributed to the effect from hilly terrain on agriculture outside the floodplain. Furthermore, among these 24 counties with significant NDVI deficit, 19 exhibit a significant downward trend in NDVI deficit (Fig. 3d). Observations also indicate a substantial reduction in NDVI deficit across all 4 sub-regions, with upstream and south-bank counties experienced a more substantial and sharp decrease (Fig. 3d, Fig. S2). This spatial variation in decrease rate of NDVI deficit correlates with stabilization in riverine hydrology at the sub-regional scale (Fig. 2d, Fig. 3).

3.3. Increased proximity of human activity and river

The distance between human activities and the river has undergone dramatic changes, mostly decreasing after the 2000s. The average distance between newly-cultivated cropland and the river shows an increase-decrease trend, with an average reduction rate of $28.88 \text{ m year}^{-1}$ (Fig. 4a). The average distance is 1258 m during 2010–2021, which is 16% less than that of 1998–2009 (1492 m) but still significantly larger than that during 1987–1997 (939 m). The average riverine distance of newly-emerged settlements is 2794 m, nearly twice that of newly-cultivated cropland. It witnessed a continuous decrease during 1987–2015, with an average rate of $34.63 \text{ m year}^{-1}$ (Fig. 4a). Human-water distance has gotten closer, particularly after 2000.

The spatial distribution of agriculture in the LYRF is also influenced by the river and its dynamic (Fig. 4b and c). The average NDVI on cropland maintains a consistent positive correlation with the distance to water, indicating the deficit of agricultural productivity near the river (Fig. 4c). However, there is an observed upward trend in average NDVI across all buffer zones, with the closest rings experiencing the strongest increase (Fig. 4c). Additionally, the NDVI gradient is calculated using linear regression on the average NDVI in riverine buffer rings (30 rings),

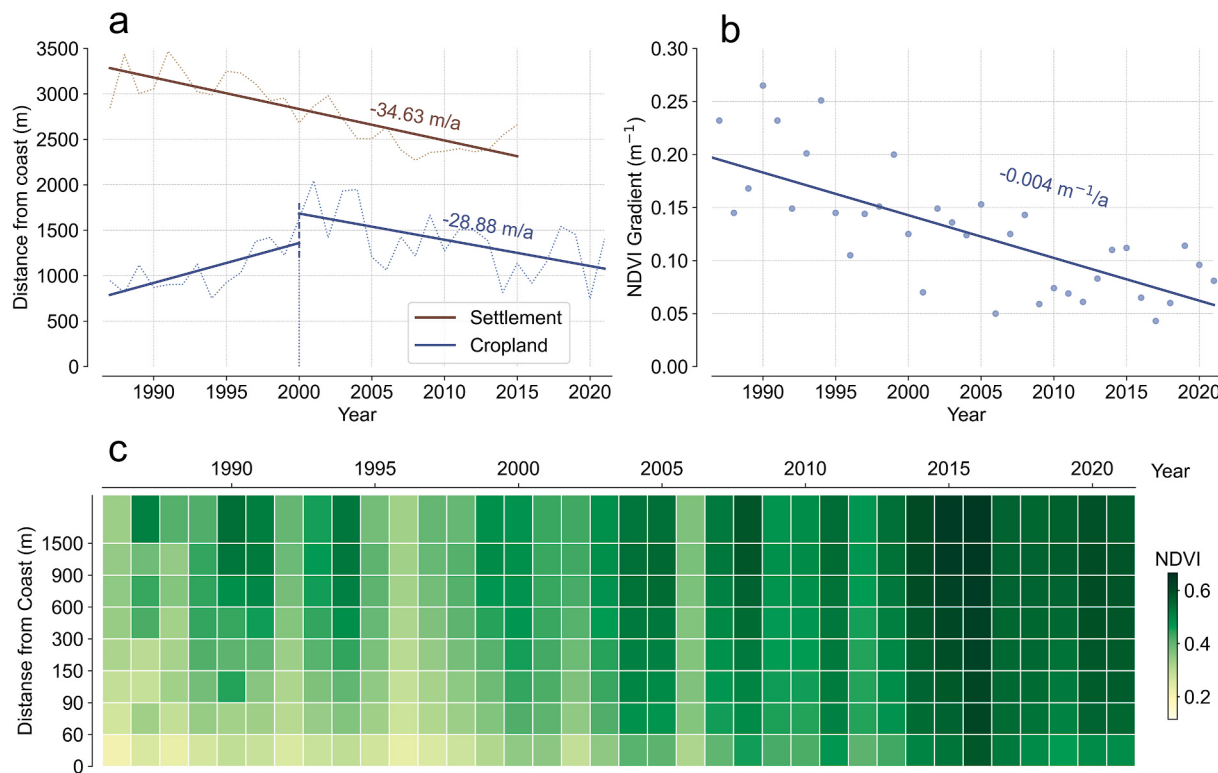


Fig. 4. Proximity of human activity and river. (a) Average distance from newly-cultivated cropland & newly-emerged settlement to the river. (b) Time sequence of NDVI gradient (30 rings \times 30 m). (c) Average NDVI on cropland in riverine buffer rings.

each 30 m in width) against their respective distances from the river. This measure quantifies the rate of agricultural intensity decline as one approaches the river. The NDVI gradient has experienced a significant decline, with a 60% decrease from 1986 to 1997 to 2010–2021 (Fig. 4b), indicating that the sensitivity of agriculture in the LYRF to its distance from the riverbank has decreased.

3.4. Linkage between river stabilization and agriculture activities

The above results have illustrated the dynamics of floodplain human-nature interactions: a reduction in NDVI deficit in the LYRF, an increase in absolute NDVI especially in regions near the river, and a decreased distance between cropland, settlements, and the river (Fig. 5). Furthermore, the substantial riverine influence on agriculture within the LYRF is evidenced by the correlation between water-associated factors and agricultural indicators. From 1986 to 2021, both NDVI deficit and NDVI gradient within the LYRF are strongly positively correlated with seasonal surface water extent, seasonal inundated extent and permanent water migration rate, with 5 of the 6 correlations passed BLR (Fig. 6). For both agriculture variables, inundated extent exhibits a more dominate influencing evidence (as shown by larger BF₁₀) than surface water extent or migration rate, indicating a more substantial effect from the former. Correlation between water-associated factors and NDVI deficit is also found within all 4 sub-regions, with stronger evidence found in 2 Henan-regions and from inundated extent (Fig. S3). These results affirm that a larger surface water extent, more intense river diversion and more substantial inundation are linked with lower intensity of agriculture within the LYRF compared to areas outside, and a greater agricultural disparity within the floodplain between croplands nearest to the river and those further away. This explains the simultaneous and same-location occurrence of agricultural intensification and river stabilization.

4. Discussion

Understanding hydrological influences on human-nature interactions is crucial for effective management, particularly in flood-prone regions like the LYRF. This study analyzed the hydrological changes of the LYR, significant agricultural deficit, intensification and spatial variation in the LYRF from 1986 to 2021, and established a connection between the river's stabilization and floodplain human-nature interaction. Over this period, the natural flood-prone characteristic of the LYR has diminished, as evidenced by the consistent decrease in seasonal water bodies and the decline in annual maximum water extent after 2004. Simultaneously, the river's channel has exhibited stabilization, with the migration rate reducing after 1996. Accompanied by these shifts, noticeable changes in human-nature interactions within the less-developed LYRF region have unfolded, demonstrated by increased NDVI and reduced NDVI deficit. Changes in spatial patterns of the human-nature interaction have also been identified, characterized notably by a closer proximity to rivers and heightened development in river-adjacent areas.

Situated near the unstable LYR, human-nature interactions in the LYRF are heavily influenced by river hydrology. Due to insufficient flood protection, cultivation within the floodplain is particularly vulnerable, especially near the river (Zhang et al., 2020). On the contrary, the presence of levees can eliminate this risk, thus having no impact on agriculture outside the floodplain. Consequently, less investment was allocated to cropland within the LYRF, resulting in lower productivity coupled with actual flood losses (Fig. 7a). Similarly, the closer proximity to the river increases the likelihood of inundation, leading to lower agricultural intensity near the riverbanks and creating distinct NDVI gradients. Settlements, requiring additional flood protection and holding higher value, are consequently situated farther from the river (Fig. 7a). However, with the stabilization of the LYR, there has been a noticeable shift in the pattern of floodplain human-nature interaction.

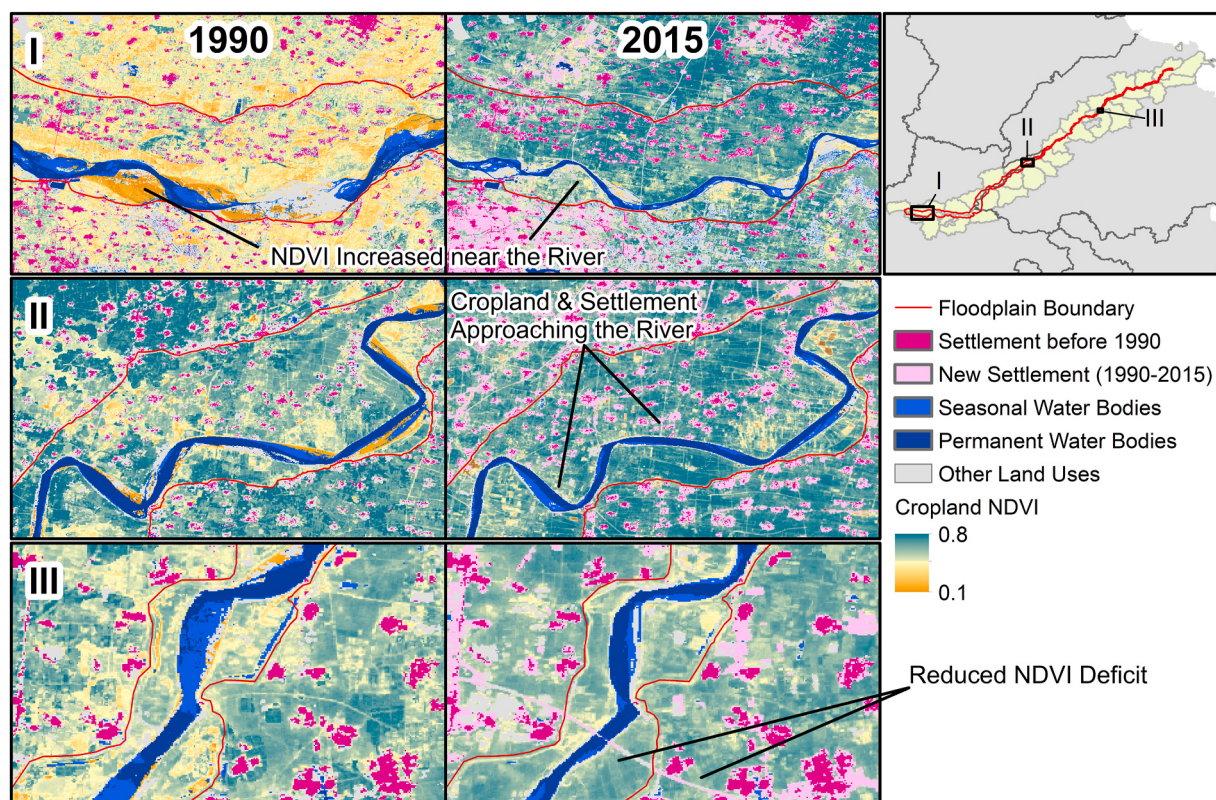


Fig. 5. Illustration of different kind of human-nature interactions changes in the LYRF. (I) Absolute NDVI in the floodplain and riverine region increased. (II) Cropland and settlement approached the river. (III) NDVI deficit inside floodplain has reduced.

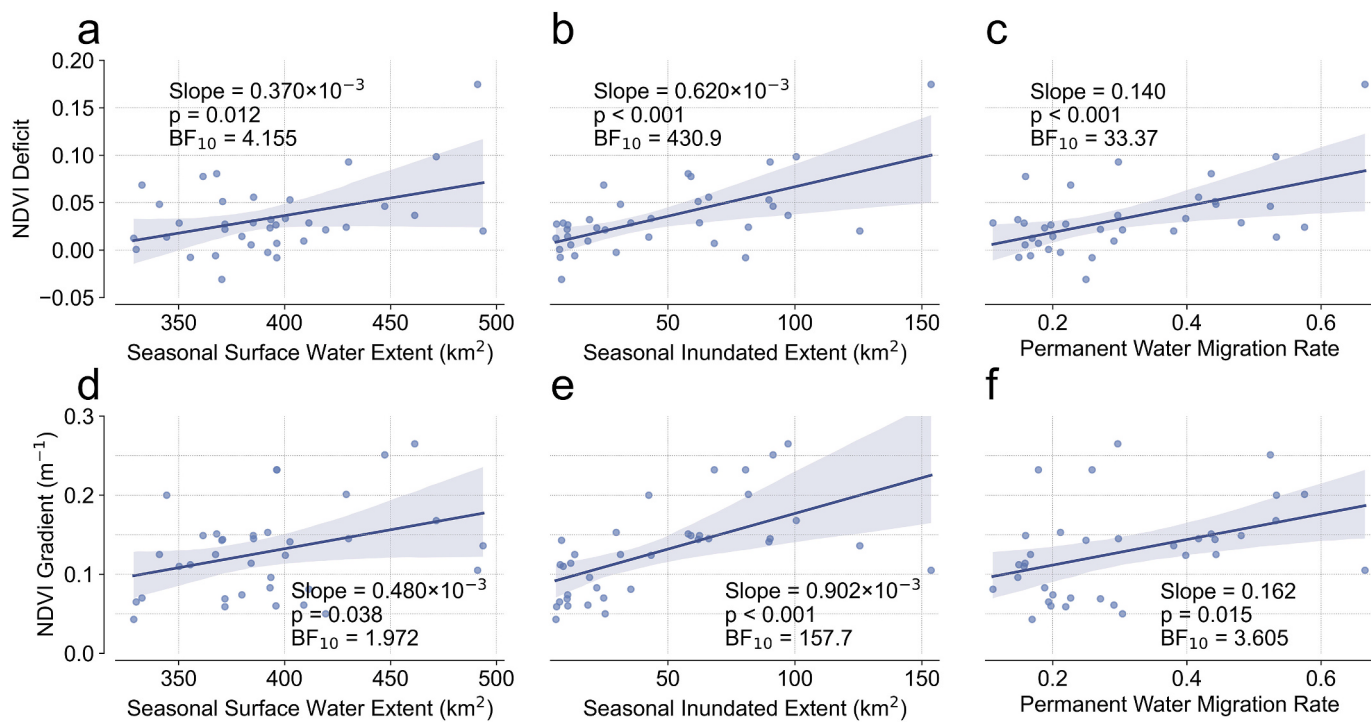


Fig. 6. Correlations between water-associated factors and NDVI Deficit/NDVI Gradient (shadows show 95% creditable interval of classical linear regressions).

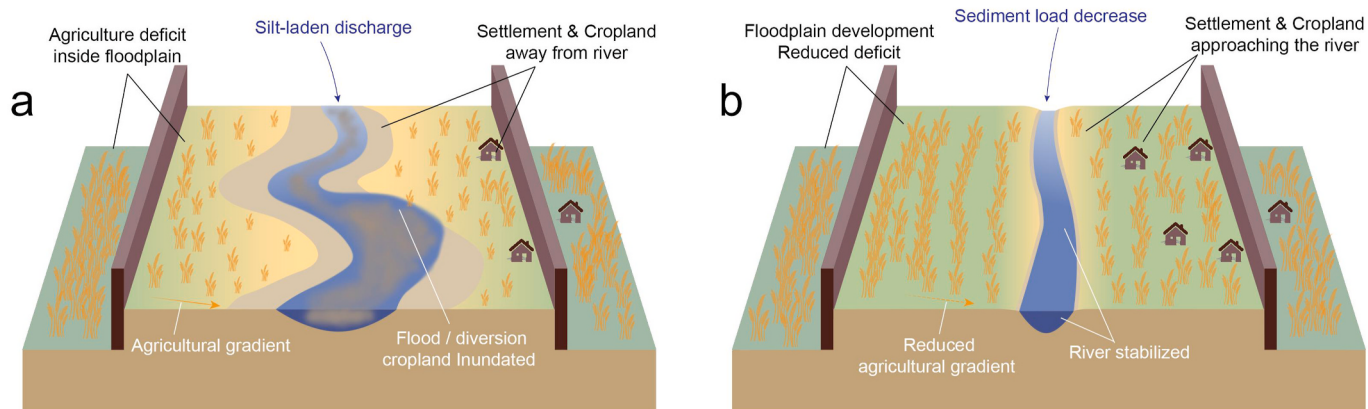


Fig. 7. Human-nature interaction patterns in the LYRF. (a) Before river stabilization. (b) After river stabilization.

As the extent of water bodies has decreased and the river's stability has improved, the risk of inundation has diminished, prompting investment in cropland within the floodplain and along the underdeveloped coastal areas to maximize output. Consequently, agricultural intensity within the floodplain has surged, and distance minimized between agricultural operations and the river (Fig. 7b). Notably, the upper-reach counties, which were more severely affected by the river's wandering and flooding (Wu et al., 2023), have seen significant decrease in water and flooded extent and experienced more substantial transformation. The narrower floodplain in lower-reach SdS counties has been found to exhibit stronger evidence of river migration's impact on NDVI deficit (see Fig. S3), and it appears to have benefited more from stabilization of the river channel.

The river's stabilization, which led to the transformation of floodplain human-nature interactions, can be attributed to channel deepening and an increase in bankfull discharge (Kong et al., 2015; Xia et al., 2014). In the LYR, the relationship between flood season discharge and seasonal water bodies exhibited a marked difference between 1986–1998 and 2010–2021, with a similar discharge producing less

surface water (Fig. S4a). Likewise, the relationship between flood season discharge and seasonally inundated extent has also changed, resulting in significantly fewer croplands being inundated by a similar discharge (Fig. S4b). Water regulation practices above the LYRB have played a crucial role. The Grain for Green Program, initiated in the Loess Plateau in 1999, has successfully reduced soil erosion and decreased sediment input to the Yellow River (Feng et al., 2016; Wang et al., 2016), alleviating the silt-up problem of river channel. The Xiaolangdi Reservoir, located upstream of the LYRB and operational since 2002, has been conducting runoff and sediment control (Wang et al., 2017a,b; Yang et al., 2008). Regulation from the reservoir not only reduces extreme flood but also alters nature allocation of sediment load to facilitate downstream channel deepening (Peng et al., 2010; Yang et al., 2008). Therefore, the LYRF serves as a typical example of how upstream river management, including erosion management and reservoir operation, can lead to river stabilization and further agricultural development in the downstream floodplain (Kong et al., 2020; Wang et al., 2019; Wu et al., 2023). Similar effects from upstream practices to downstream human-nature interactions have also been reported globally. In the

Mekong River Basin, upstream hydropower development has resulted in losses in floodplain fisheries and delta rice agriculture (Chapman et al., 2016; Ziv et al., 2012). In Bangladesh, the influence of upstream water withdrawal on downstream land use and livelihoods has been documented (Ahmed et al., 2022). Hence, the findings of this study underscore the importance of integrated basin management (Best, 2019; Molle, 2009; Wu and Whittington, 2006), urging not merely a focus on local impacts, but also consideration of spillover effects on the entire basin.

Enhanced agricultural intensity within the LYRF may present both new opportunities and challenges for floodplain management. The current policy of relocating floodplain residents outward has encountered challenges due to an extreme shortage of land resources (Zhang et al., 2022). However, the enduring stability of the river provides favorable conditions for human activities, unlocking productivity potential that was previously constrained by flood risk. Despite recent advancements, an agricultural deficit persists within the LYRF, suggesting untapped agricultural potential still exists. However, the future trajectory of the LYR remains uncertain, as current estimations on flood characteristics of the LYR are inconclusive, even in terms of basic discharge trend (Bai et al., 2016; Ji et al., 2021; Zhao et al., 2019). The phenomenon of "levee effect" posits that the levee construction may reduce people's awareness of flood risk, promote development in the floodplain and result in severe losses during future flood events (Collenteur et al., 2015; Di Baldassarre et al., 2018; Ding et al., 2023; White, 1945). In the LYRF, river stabilization could have had a similar effect, reducing flood perception in much the same way as levee construction. Consequently, flood risk control must be primarily considered during floodplain management, for which optimization of human-nature interactions is needed. In the upper floodplains that are rarely reached by floods, agriculture and residence can be promoted to fully utilize land resources. Conversely, the river channel and the lower floodplains, which serve primary flood discharge functions, should be protected against anthropogenic utilization (Ahrendt et al., 2022; Gori et al., 2019; Mijic et al., 2023). Moreover, current measures of farm dikes in the floodplain could also be reinforced to increase the floodplain agriculture's resilience to flooding (Wu et al., 2023).

5. Conclusion

This study examines the impact of riverine hydrological changes on floodplain human-nature interactions using the Lower Yellow River Floodplain as a case study. It quantifies hydrological change with open-surface water extent, and human activities in terms of area and intensity based on long-term remote sensing-based datasets. The results of this study suggests that the agriculture within the floodplain has been affected by the flood risk of the Lower Yellow River, with its intensity significantly lower than outside. However, as the river has experienced stabilization since the 1990s, the agriculture within the floodplain has witnessed flourish, as the intensity of agriculture increased faster than outside, and human-river distance decreased in the floodplain. Findings of this study emphasizes the importance of integrated basin management on floodplain development. This study attributes the stabilization of the Lower Yellow River to upstream river regulation practices based on existing literatures, and further studies are encouraged to establish a quantitative relationship between floodplain human-nature interaction and river regulation efforts. Moreover, hydrological projection method may also be utilized to explore floodplain human-nature interactions in the context of future climate change.

CRediT authorship contribution statement

Chentai Jiao: Writing – original draft, Visualization, Methodology, Formal analysis, Conceptualization. **Xutong Wu:** Writing – review & editing, Project administration, Methodology, Funding acquisition, Conceptualization. **Shuang Song:** Writing – review & editing,

Visualization. **Shuai Wang:** Writing – review & editing, Supervision, Project administration, Funding acquisition. **Bei Xiang:** Validation. **Bojie Fu:** Supervision, Resources, Project administration, Funding acquisition.

Code availability

Code used in this study in Python and JavaScript (for Google Earth Engine) is available upon reasonable request.

Declaration of competing interest

The authors declare that they have no known competing financial interests or personal relationships that could have appeared to influence the work reported in this paper.

Acknowledgements

This research has been supported by the National Natural Science Foundation of China (grant no. U2243601, 42041007 and 42201306) and the Fundamental Research Funds for the Central Universities.

Appendix A. Supplementary data

Supplementary data to this article can be found online at <https://doi.org/10.1016/j.jenvman.2024.122957>.

Data availability

Landsat dataset used to extract open-surface water bodies and NDVI is acquired from Google Earth Engine (<https://developers.google.com/earth-engine/datasets/catalog/landsat>). CACD dataset is derived from Zenodo (<https://zenodo.org/records/7936885>). WSFE dataset is derived from EOC Geoservice (https://download.geoservice.dlr.de/WSF_EVO/). Runoff of the LYR is derived from the Yellow River Conservancy Commission (<http://www.yrcc.gov.cn/>, in Chinese).

References

- Aerts, J.C.J.H., Bates, P.D., Botzen, W.J.W., de Bruijn, J., Hall, J.W., van den Hurk, B., Kreibich, H., Merz, B., Muis, S., Mysiak, J., Tate, E., Berkhouwt, F., 2024. Exploring the limits and gaps of flood adaptation. *Nat. Water* 2, 719–728. <https://doi.org/10.1038/s44221-024-00274-x>.
- Ahmed, Z., Alam, R., Ahmed, M.N.Q., Ambinakudige, S., Almazroui, M., Islam, M.N., Chowdhury, P., Kabir, MdN., Mahmud, S., 2022. Does anthropogenic upstream water withdrawal impact on downstream land use and livelihood changes of Teesta transboundary river basin in Bangladesh? *Environ. Monit. Assess.* 194, 59. <https://doi.org/10.1007/s10661-021-09726-3>.
- Ahrendt, S., Horner-Devine, A.R., Collins, B.D., Morgan, J.A., Istanbulluoglu, E., 2022. Channel conveyance variability can influence flood risk as much as streamflow variability in Western Washington state. *Water Resour. Res.* 58, e2021WR031890. <https://doi.org/10.1029/2021WR031890>.
- Amrhein, V., Greenland, S., McShane, B., 2019. Scientists rise up against statistical significance. *Nature* 567, 305–307. <https://doi.org/10.1038/d41586-019-00857-9>.
- Andreadis, K.M., Wing, O.E.J., Colven, E., Gleason, C.J., Bates, P.D., Brown, C.M., 2022. Urbanizing the floodplain: global changes of imperviousness in flood-prone areas. *Environ. Res. Lett.* 17, 104024. <https://doi.org/10.1088/1748-9326/ac9197>.
- Bai, P., Liu, X., Liang, K., Liu, C., 2016. Investigation of changes in the annual maximum flood in the Yellow River basin, China. *Quat. Int., Paleoenvironmental studies in the Korean Peninsula and adjacent geographic areas IV* 392, 168–177. <https://doi.org/10.1016/j.quaint.2015.04.053>.
- Barendrecht, M.H., Viglione, A., Kreibich, H., Merz, B., Vorogushyn, S., Blöschl, G., 2019. The value of Empirical data for estimating the parameters of a sociohydrological flood risk model. *Water Resour. Res.* 55, 1312–1336. <https://doi.org/10.1029/2018WR024128>.
- Best, J., 2019. Anthropogenic stresses on the world's big rivers. *Nat. Geosci.* 12, 7–21. <https://doi.org/10.1038/s41561-018-0262-x>.
- Black, R., Bennett, S.R.G., Thomas, S.M., Beddington, J.R., 2011. Migration as adaptation. *Nature* 478, 447–449. <https://doi.org/10.1038/478477a>.
- Bryan, K., 1923. Erosion and sedimentation in the Papago country, Arizona, with a sketch of the geology. *Bulletin*. <https://doi.org/10.3133/b730B>.
- Bubeck, P., Botzen, W.J.W., Kreibich, H., Aerts, J.C.J.H., 2013. Detailed insights into the influence of flood-coping appraisals on mitigation behaviour. *Glob. Environ. Change* 23, 1327–1338. <https://doi.org/10.1016/j.gloenvcha.2013.05.009>.

- Buchinsky, F.J., Chadha, N.K., 2017. To P or not to P: backing bayesian statistics. *Otolaryngol. Neck Surg.* 157, 915–918. <https://doi.org/10.1177/0194599817739260>.
- Chapman, A.D., Darby, S.E., Hòng, H.M., Tompkins, E.L., Van, T.P.D., 2016. Adaptation and development trade-offs: fluvial sediment deposition and the sustainability of rice-cropping in an Giang Province, Mekong Delta. *Clim. Change* 137, 593–608. <https://doi.org/10.1007/s10584-016-1684-3>.
- Charloux, G., Mahmoud, M.A.A., Elnasseh, A.M.S., Marchand, S., 2021. The shifting Nile and the origins and development of ancient Karnak. *Antiquity* 95, 919–939. <https://doi.org/10.15184/ajq.2021.73>.
- Collette, R.A., de Moel, H., Jongman, B., Di Baldassarre, G., 2015. The failed-levee effect: do societies learn from flood disasters? *Nat. Hazards* 76, 373–388. <https://doi.org/10.1007/s11069-014-1496-6>.
- Dawson, R.J., Ball, T., Werritty, J., Werritty, A., Hall, J.W., Roche, N., 2011. Assessing the effectiveness of non-structural flood management measures in the Thames Estuary under conditions of socio-economic and environmental change. *Glob. Environ. Change, Special Issue on The Politics and Policy of Carbon Capture and Storage* 21, 628–646. <https://doi.org/10.1016/j.gloenvcha.2011.01.013>.
- Deng, Y., Jiang, W., Tang, Z., Ling, Z., Wu, Z., 2019. Long-term changes of open-surface water bodies in the yangtze River Basin based on the Google Earth engine cloud platform. *Remote Sens* 11, 2213. <https://doi.org/10.3390/rs11192213>.
- Devitt, L., Neal, J., Coxon, G., Savage, J., Wagener, T., 2023. Flood hazard potential reveals global floodplain settlement patterns. *Nat. Commun.* 14, 2801. <https://doi.org/10.1038/s41467-023-38297-9>.
- Di Baldassarre, G., Kooy, M., Kemerink, J.S., Brandimarte, L., 2013a. Towards understanding the dynamic behaviour of floodplains as human-water systems. *Hydrol. Earth Syst. Sci.* 17, 3235–3244. <https://doi.org/10.5194/hess-17-3235-2013>.
- Di Baldassarre, G., Viglione, A., Carr, G., Kuil, L., Salinas, J.L., Blöschl, G., 2013b. Socio-hydrology: conceptualising human-flood interactions. *Hydrol. Earth Syst. Sci.* 17, 3295–3303. <https://doi.org/10.5194/hess-17-3295-2013>.
- Di Baldassarre, G., Kreibich, H., Vorogushyn, S., Aerts, J., Arnbjerg-Nielsen, K., Barendrecht, M., Bates, P., Borga, M., Botzen, W., Bubeck, P., De Marchi, B., Llasat, C., Mazzoleni, M., Molinari, D., Mondino, E., Mård, J., Petrucci, O., Scolobig, A., Viglione, A., Ward, P.J., 2018. Hess Opinions: an interdisciplinary research agenda to explore the unintended consequences of structural flood protection. *Hydrol. Earth Syst. Sci.* 22, 5629–5637. <https://doi.org/10.5194/hess-22-5629-2018>.
- Di Baldassarre, G., Sivapalan, M., Rusca, M., Cudennec, C., Garcia, M., Kreibich, H., Konar, M., Mondino, E., Mård, J., Pandey, S., Sanderson, M.R., Tian, F., Viglione, A., Wei, J., Wei, Y., Yu, D.J., Srinivasan, V., Blöschl, G., 2019. Sociohydrology: scientific challenges in addressing the sustainable development goals. *Water Resour. Res.* 55, 6327–6355. <https://doi.org/10.1029/2018WR023901>.
- Ding, M., Lin, P., Gao, S., Wang, J., Zeng, Z., Zheng, K., Zhou, X., Yamazaki, D., Gao, Y., Liu, Y., 2023. Reversal of the levee effect towards sustainable floodplain management. *Nat. Sustain.* 6, 1578–1586. <https://doi.org/10.1038/s41893-023-01202-9>.
- Fang, Y., Du, S., Wen, J., Zhang, M., Fang, J., Liu, M., 2021. Chinese built-up land in floodplains moving closer to freshwaters. *Int. J. Disaster Risk Sci.* 12, 355–366. <https://doi.org/10.1007/s13753-021-00343-9>.
- Feng, X., Fu, B., Piao, S., Wang, S., Ciais, P., Zeng, Z., Lü, Y., Zeng, Y., Li, Y., Jiang, X., Wu, B., 2016. Revegetation in China's Loess Plateau is approaching sustainable water resource limits. *Nat. Clim. Change* 6, 1019–1022. <https://doi.org/10.1038/nclimate3092>.
- Fu, B., Wang, S., Liu, Y., Liu, J., Liang, W., Miao, C., 2017. Hydrogeomorphic ecosystem responses to natural and anthropogenic changes in the Loess Plateau of China. *Annu. Rev. Earth Planet Sci.* 45, 223–243. <https://doi.org/10.1146/annurev-earth-063016-020552>.
- Gori, A., Blessing, R., Juan, A., Brody, S., Bedient, P., 2019. Characterizing urbanization impacts on floodplain through integrated land use, hydrologic, and hydraulic modeling. *J. Hydrol.* 568, 82–95. <https://doi.org/10.1016/j.jhydrol.2018.10.053>.
- Güneralp, B., Güneralp, İ., Liu, Y., 2015. Changing global patterns of urban exposure to flood and drought hazards. *Glob. Environ. Change* 31, 217–225. <https://doi.org/10.1016/j.gloenvcha.2015.01.002>.
- Hino, M., Field, C.B., Mach, K.J., 2017. Managed retreat as a response to natural hazard risk. *Nat. Clim. Change* 7, 364–370. <https://doi.org/10.1038/nclimate3252>.
- Hoyt, W.G., Langbein, W.B., 1955. *Floods*. Princeton University Press, Princeton, NJ.
- Ji, G., Lai, Z., Xia, H., Liu, H., Wang, Z., 2021. Future runoff variation and flood disaster prediction of the Yellow River Basin based on CA-markov and SWAT. *Land* 10, 421. <https://doi.org/10.3390/land10040421>.
- Jiao, C., Wang, S., Song, S., Fu, B., 2023. Long-term and seasonal variation of open-surface water bodies in the Yellow River Basin during 1990–2020. *Hydrol. Process.* 37, e14846. <https://doi.org/10.1002/hyp.14846>.
- Jongman, B., Ward, P.J., Aerts, J.C.J.H., 2012. Global exposure to river and coastal flooding: long term trends and changes. *Glob. Environ. Change* 22, 823–835. <https://doi.org/10.1016/j.gloenvcha.2012.07.004>.
- Jongman, B., Winsemius, H.C., Aerts, J.C.J.H., Coughlan de Perez, E., van Aalst, M.K., Kron, W., Ward, P.J., 2015. Declining vulnerability to river floods and the global benefits of adaptation. *Proc. Natl. Acad. Sci.* 112, E2271–E2280. <https://doi.org/10.1073/pnas.1414439112>.
- Kong, D., Latrubesse, E.M., Miao, C., Zhou, R., 2020. Morphological response of the lower Yellow River to the operation of xiaolangdi dam, China. *Geomorphology* 350, 106931. <https://doi.org/10.1016/j.geomorph.2019.106931>.
- Kong, D., Miao, C., Wu, J., Duan, Q., Sun, Q., Ye, A., Di, Z., Gong, W., 2015. The hydro-environmental response on the lower Yellow River to the water-sediment regulation scheme. *Ecol. Eng.* 79, 69–79. <https://doi.org/10.1016/j.ecoleng.2015.03.009>.
- Li, J., Lu, Y., Li, X., Wang, R., Sun, Y., Liu, Y., Yao, K., 2023. Evaluation and analysis of development status of Yellow River beach area based on multi-source data and coordination degree model. *Sustainability* 15, 6086. <https://doi.org/10.3390/su15076086>.
- Li, L., Shen, H., Dai, S., Xiao, J., Shi, X., 2012. Response of runoff to climate change and its future tendency in the source region of Yellow River. *J. Geogr. Sci.* 22, 431–440. <https://doi.org/10.1007/s11442-012-0937-y>.
- Liu, Y., Wang, E., Yang, X., Wang, J., 2010. Contributions of climatic and crop varietal changes to crop production in the North China Plain, since 1980s. *Glob. Change Biol.* 16, 2287–2299. <https://doi.org/10.1111/j.1365-2486.2009.02077.x>.
- Marconcini, M., Gorelick, N., Metz-Marconcini, A., Esch, T., 2020a. Accurately monitoring urbanization at global scale – the world settlement footprint. *IOP Conf. Ser. Earth Environ. Sci.* 509, 012036. <https://doi.org/10.1088/1755-1315/509/1/012036>.
- Marconcini, Mattia, Metz-Marconcini, A., Üreyen, S., Palacios-Lopez, D., Hanke, W., Bachofner, F., Zeidler, J., Esch, T., Gorelick, N., Kakarla, A., Paganini, M., Strano, E., 2020b. Outlining where humans live, the world settlement footprint 2015. *Sci. Data* 7, 242. <https://doi.org/10.1038/s41597-020-00580-5>.
- Mazzoleni, M., Mård, J., Rusca, M., Odongo, V., Lindersson, S., Di Baldassarre, G., 2021. Floodplains in the anthropocene: a global analysis of the interplay between human population, built environment, and flood severity. *Water Resour. Res.* 57, e2020WR027744. <https://doi.org/10.1029/2020WR027744>.
- Mijic, A., Liu, L., O'Keeffe, J., Dobson, B., Chun, K.P., 2023. A meta-model of socio-hydrological phenomena for sustainable water management. *Nat. Sustain.* 1–8. <https://doi.org/10.1038/s41893-023-01240-3>.
- Molle, F., 2009. River-basin planning and management: the social life of a concept. *GeoForum, Themed Issue: Gramscian Political Ecologies* 40, 484–494. <https://doi.org/10.1016/j.geoforum.2009.03.004>.
- Pekel, J.-F., Cottam, A., Gorelick, N., Belward, A.S., 2016. High-resolution mapping of global surface water and its long-term changes. *Nature* 540, 418–422. <https://doi.org/10.1038/nature20584>.
- Peng, J., Chen, S., Dong, P., 2010. Temporal variation of sediment load in the Yellow River basin, China, and its impacts on the lower reaches and the river delta. *Catena* 83, 135–147. <https://doi.org/10.1016/j.catena.2010.08.006>.
- Rajib, A., Zheng, Q., Lane, C.R., Golden, H.E., Christensen, J.R., Isibor, I.I., Johnson, K., 2023. Human alterations of the global floodplains 1992–2019. *Sci. Data* 10, 499. <https://doi.org/10.1038/s41597-023-02382-x>.
- Ringler, C., Cai, X., Wang, J., Ahmed, A., Xue, Y., Xu, Z., Yang, E., Jianshi, Z., Zhu, T., Cheng, L., Yongfeng, F., Xinfeng, F., Xiaowei, G., You, L., 2010. Yellow River basin: living with scarcity. *Water Int.* 35, 681–701. <https://doi.org/10.1080/02508060.2010.509857>.
- Rufat, S., Tate, E., Burton, C.G., Maroof, A.S., 2015. Social vulnerability to floods: review of case studies and implications for measurement. *Int. J. Disaster Risk Reduct.* 14, 470–486. <https://doi.org/10.1016/j.ijdrr.2015.09.013>.
- Run, Y., Li, M., Qin, Y., Shi, Z., Li, Q., Cui, Y., 2022. Dynamics of land and water resources and utilization of cultivated land in the Yellow River beach area of China. *Water* 14, 305. <https://doi.org/10.3390/w14030305>.
- Schmidt, G., Jenkerson, C., Masek, J., Vermote, E., Gao, F., 2013. Landsat Ecosystem Disturbance Adaptive Processing System (LEDAPS) Algorithm Description (No. 2013-1057), Open-File Report. U.S. Geological Survey.
- Schober, B., Hauer, C., Habersack, H., 2020. Floodplain losses and increasing flood risk in the context of recent historic land use changes and settlement developments: Austrian case studies. *J. Flood Risk Manag.* 13, e12610. <https://doi.org/10.1111/jfr3.12610>.
- Schönbrodt, F.D., Wagenmakers, E.-J., 2018. Bayes factor design analysis: planning for compelling evidence. *Psychon. Bull. Rev.* 25, 128–142. <https://doi.org/10.3758/s13423-017-1230-y>.
- Song, S., Wang, S., Fu, B., Dong, Y., Liu, Y., Chen, H., Wang, Y., 2021. Improving representation of collective memory in socio-hydrological models and new insights into flood risk management. *J. Flood Risk Manag.* 14, e12679. <https://doi.org/10.1111/jfr3.12679>.
- Song, S., Wang, S., Fu, B., Liu, Y., Wang, K., Li, Y., Wang, Y., 2020. Sediment transport under increasing anthropogenic stress: regime shifts within the Yellow River, China. *Ambio* 49, 2015–2025. <https://doi.org/10.1007/s13280-020-01350-8>.
- Song, S., Wen, H., Wang, S., Wu, X., Cumming, G.S., Fu, B., 2024. Quantifying the effects of institutional shifts on water governance in the Yellow River Basin: a social-ecological system perspective. *J. Hydrol.* 629, 130638. <https://doi.org/10.1016/j.jhydrol.2024.130638>.
- Tanoue, M., Taguchi, R., Alifu, H., Hirabayashi, Y., 2021. Residual flood damage under intensive adaptation. *Nat. Clim. Change* 11, 823–826. <https://doi.org/10.1038/s41588-021-01158-8>.
- Tockner, K., Stanford, J.A., 2002. Riverine flood plains: present state and future trends. *Environ. Conserv.* 29, 308–330. <https://doi.org/10.1017/S037689290200022X>.
- Tu, Y., Wu, S., Chen, B., Weng, Q., Gong, P., Bai, Y., Yang, J., Yu, L., Xu, B., 2023. A 30 m annual cropland dataset of China from 1986 to 2021. *Earth Syst. Sci. Data Discuss.* 1–34. <https://doi.org/10.5194/essd-2023-190>.
- van den Bergh, D., Clyde, M.A., Gupta, A.R.K.N., de Jong, T., Gronau, Q.F., Marsman, M., Ly, A., Wagenmakers, E.-J., 2021. A tutorial on Bayesian multi-model linear regression with BAS and JASP. *Behav. Res. Methods* 53, 2351–2371. <https://doi.org/10.3758/s13428-021-01552-2>.
- Wakefield, J., 2009. Bayes factors for genome-wide association studies: comparison with P-values. *Genet. Epidemiol.* 33, 79–86. <https://doi.org/10.1002/gepi.20359>.
- Wang, H., Sun, F., 2021. Variability of annual sediment load and runoff in the Yellow River for the last 100 years (1919–2018). *Sci. Total Environ.* 758, 143715. <https://doi.org/10.1016/j.scitotenv.2020.143715>.

- Wang, H., Wu, X., Bi, N., Li, S., Yuan, P., Wang, A., Syvitski, J.P.M., Saito, Y., Yang, Z., Liu, S., Nittrouer, J., 2017b. Impacts of the dam-oriented water-sediment regulation scheme on the lower reaches and delta of the Yellow River (Huanghai): a review. *Glob. Planet. Change* 157, 93–113. <https://doi.org/10.1016/j.gloplacha.2017.08.005>.
- Wang, N., Sun, F., Yang, S., Liu, W., Wang, H., 2024. The heterogeneity of human flood adaptation characteristics in Central Asia based on human-flood distance. *Environ. Res. Lett.* 19, 064061. <https://doi.org/10.1088/1748-9326/ad4b43>.
- Wang, S., Fu, B., Liang, W., Liu, Y., Wang, Y., 2017a. Driving forces of changes in the water and sediment relationship in the Yellow River. *Sci. Total Environ.* 576, 453–461. <https://doi.org/10.1016/j.scitotenv.2016.10.124>.
- Wang, S., Fu, B., Piao, S., Lü, Y., Ciais, P., Feng, X., Wang, Y., 2016. Reduced sediment transport in the Yellow River due to anthropogenic changes. *Nat. Geosci.* 9, 38–41. <https://doi.org/10.1038/ngeo2602>.
- Wang, Y., Zhao, W., Wang, S., Feng, X., Liu, Y., 2019. Yellow River water rebalanced by human regulation. *Sci. Rep.* 9, 1–10. <https://doi.org/10.1038/s41598-019-46063-5>.
- Wang, Z., Liu, C., 2019. Two-thousand years of debates and practices of Yellow River training strategies. *Int. J. Sediment Res.* 34, 73–83. <https://doi.org/10.1016/j.ijscsr.2018.08.006>.
- White, G.F., 1945. *Human Adjustment to Floods*. The University of Chicago, Chicago, IL.
- Wu, C., 1991. On the core of geographical research—the regional system human-nature relationship. *Econ. Geogr.* 1–6 (Chinese).
- Wu, X., Feng, X., Fu, B., Yin, S., He, C., 2023. Managing erosion and deposition to stabilize a silt-laden river. *Sci. Total Environ.* 881, 163444. <https://doi.org/10.1016/j.scitotenv.2023.163444>.
- Wu, X., Whittington, D., 2006. Incentive compatibility and conflict resolution in international river basins: a case study of the Nile Basin. *Water Resour. Res.* 42, <https://doi.org/10.1029/2005WR004238>.
- Xia, J., Li, X., Zhang, X., Li, T., 2014. Recent variation in reach-scale bankfull discharge in the Lower Yellow River. *Earth Surf. Process. Landf.* 39, 723–734. <https://doi.org/10.1002/esp.3474>.
- Xu, J., Ma, Y., 2009. Response of the hydrological regime of the Yellow River to the changing monsoon intensity and human activity. *Hydrol. Sci. J.* 54, 90–100. <https://doi.org/10.1623/hysj.54.1.90>.
- Yang, T., Zhang, Q., Chen, Y.D., Tao, X., Xu, C., Chen, X., 2008. A spatial assessment of hydrologic alteration caused by dam construction in the middle and lower Yellow River, China. *Hydrol. Process.* 22, 3829–3843. <https://doi.org/10.1002/hyp.6993>.
- Zhang, J., Shang, Y., Cui, M., Luo, Q., Zhang, R., 2022. Successful and sustainable governance of the lower Yellow River, China: a floodplain utilization approach for balancing ecological conservation and development. *Environ. Dev. Sustain.* 24, 3014–3038. <https://doi.org/10.1007/s10668-021-01593-9>.
- Zhang, J., Shang, Y., Liu, J., Fu, J., Cui, M., 2020. Improved ecological development model for lower Yellow River floodplain, China. *Water Sci. Eng.* 13, 275–285. <https://doi.org/10.1016/j.wse.2020.12.006>.
- Zhao, H., Xu, X., Tang, J., Wang, Z., Miao, C., 2023. Spatial pattern evolution and prediction scenario of habitat quality in typical fragile ecological region, China: a case study of the Yellow River floodplain area. *Heliyon* 9, e14430. <https://doi.org/10.1016/j.heliyon.2023.e14430>.
- Zhao, Y., Cao, W., Hu, C., Wang, Y., Wang, Z., Zhang, X., Zhu, B., Cheng, C., Yin, X., Liu, B., Xie, G., 2019. Analysis of changes in characteristics of flood and sediment yield in typical basins of the Yellow River under extreme rainfall events. *Catena* 177, 31–40. <https://doi.org/10.1016/j.catena.2019.02.001>.
- Zhu, Z., Woodcock, C.E., 2012. Object-based cloud and cloud shadow detection in Landsat imagery. *Remote Sens. Environ.* 118, 83–94. <https://doi.org/10.1016/j.rse.2011.10.028>.
- Ziv, G., Baran, E., Nam, S., Rodríguez-Iturbe, I., Levin, S.A., 2012. Trading-off fish biodiversity, food security, and hydropower in the Mekong River Basin. *Proc. Natl. Acad. Sci.* 109, 5609–5614. <https://doi.org/10.1073/pnas.1201423109>.
- Zou, Z., Dong, J., Menarguez, M.A., Xiao, X., Qin, Y., Doughty, R.B., Hooker, K.V., David Hambricht, K., 2017. Continued decrease of open surface water body area in Oklahoma during 1984–2015. *Sci. Total Environ.* 595, 451–460. <https://doi.org/10.1016/j.scitotenv.2017.03.259>.
- Zou, Z., Xiao, X., Dong, J., Qin, Y., Doughty, R.B., Menarguez, M.A., Zhang, G., Wang, J., 2018. Divergent trends of open-surface water body area in the contiguous United States from 1984 to 2016. *Proc. Natl. Acad. Sci.* 115, 3810–3815. <https://doi.org/10.1073/pnas.1719275115>.